Doping Driven $(\pi, 0)$ Nesting and Magnetic Properties of $Fe_{1+x}Te$ Superconductors

Myung Joon Han and Sergey Y. Savrasov
Department of Physics, University of California, Davis, California 95616, USA
(Received 6 April 2009; published 3 August 2009)

To understand newly discovered superconductivity in Fe-based systems, we investigate the electronic structure and magnetic properties of $Fe_{1+x}Te$ using first-principles density functional calculations. While the undoped FeTe has the same Fermi surface nested at (π, π) as in Fe arsenides, doping by ~0.5 electrons reveals a novel square-type Fermi surface showing a strong $(\pi, 0)$ nesting and leading to a different magnetic structure. Our result strongly supports the same mechanism of superconductivity in chalcogenides as in the arsenides, reconciling theory with existing experiments. The calculated magnetic interactions are found to be critically dependent on doping and notably different from the arsenides.

DOI: 10.1103/PhysRevLett.103.067001 PACS numbers: 74.70.−b, 71.18.+y, 71.20.−b, 75.25.+z

Shortly after the discovery of the novel high temperature superconductor $LaFeAsO_{1-x}F_x$ with $T_c \sim 27$ K [1], many different types of iron-based superconductors have been reported. Now the highest T_c reaches up to ~55 K [2], and there are four different structural classes: so-called 122-[3], 111-[4], and 11-type [5] structures, in addition to the 1111 type. Although a tremendous amount of research activity devoted to this field over the years has shed light on their intriguing physical properties, our understanding of superconductivity here, and its interplay with magnetism, is still far from being complete. One of the most important properties which was found in these systems is the Fermi surface nesting, whose nesting vector corresponds to the antiferromagnetic (AFM) ordering vector of the undoped magnetic phase [6–9]. Density functional theory (DFT) calculations show that all of the four classes of these materials share this common feature in their electronic structure [7,10,11], which strongly suggests the superconductivity is exotic and is mediated by spin fluctuations [9].

Along this line, one of the most interesting questions arises in the 11-type Fe chalcogenide family: Fe(S,Se,Te) [5,12–18]. In spite of their same crystal structure represented by the two-dimensional Fe square lattice and the same Fermi surface nesting predicted by DFT calculations [11], Fe chalcogenide superconductors exhibit notable differences from the arsenides. The magnetic structure found in their parent compound, $Fe_{1+x}Te$, strongly tackles the spin fluctuation theory because the experimentally observed magnetic ordering is fairly different from that of parent arsenide compounds. Although DFT calculations predict the same Fermi surface topology, a recent neutron experiment [19] shows that, at a small $x \sim 0.068$, $Fe_{1+x}Te$ has a rotated and double-stripe AFM order. Importantly, this magnetic structure cannot be matched with the (π, π) nesting as found in all the arsenide materials and predicted by previous calculations, but requires $(\pi, 0)$ nesting which has never been reported. This ''missing nesting'' remains as a puzzle in the study of Fe-based superconductors. Therefore it is not a big surprise that some papers speculate about a different superconducting mechanism for Fe chalcogenides from the arsenides, and the reinvestigation of the electronic structure and magnetic properties for $Fe_{1+x}Te$ is of crucial importance [15,20–22].

To address these issues, we study electronic structure and magnetic interactions of $Fe_{1+x}Te$ using first-principles DFT calculations. Since it is noted experimentally [19] that FeTe has always some amount of excess Fe atoms we perform doping dependent calculations to understand their effect on the electronic and magnetic properties. Our results show that $Fe_{1+x}Te$ has a different Fermi surface topology as a function of doping, and eventually a novel $(\pi, 0)$ nesting appears at a doping level of $\delta \sim 0.5$ electrons while the (π, π) nesting is largely suppressed. This $(\pi, 0)$ nesting exactly matches with the double-stripe AFM order found in neutron experiments. Our result strongly supports the spin fluctuation mediated superconductivity for Fe chalcogenides, reconciling theory to existing experiments which showed significant differences between pnictides and chalcogenides. It is also found that magnetic interactions depend on doping, and, at the same level of doping $\delta \sim 0.5$, the calculated exchange couplings become consistent with the double-stripe phase. While the second nearest neighbor AFM coupling (J_{2a}) is strongest, the first (J_{1b}) and second neighbor ferromagnetic (FM) interactions (J_{2b}) are also significant, which is different from arsenides.

We performed the first-principles DFT calculations within local density approximation (LDA) for the exchange-correlation energy functionals [23]. The full potential linearized-muffin-tin-orbital (LMTO) method has been used [24]. To estimate the exchange interaction strengths between Fe moments, we performed a linear response calculation [25–27], which has been successfully applied earlier to $3d$ transition-metal oxides, $5f$ metallic alloys [27,28], and the other Fe arsenides [29]. To simulate electron doping a rigid-band approximation is utilized. The calculation of band dispersions, Fermi surfaces, and Stoner response functions have been done with the nonmagnetic unit cell (dotted squares in Fig. 1) and using experimental lattice parameters as in the previous study [11]. To estimate the exchange constants we performed a spin-polarized

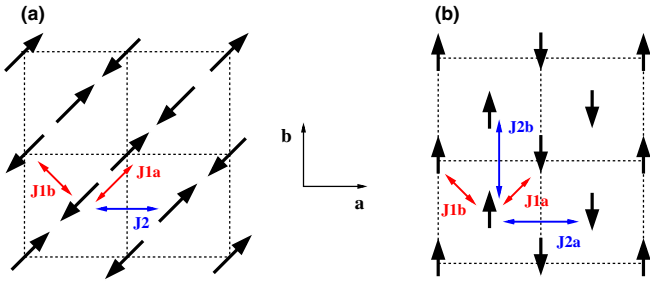

FIG. 1 (color online). The schematic picture of spin structure for (a) iron arsenide parent materials and (b) FeTe. The dotted squares correspond to the nonmagnetic unit cell and the arrows represent the spin directions. The J_{1a}, J_{1b}, J_{2a}, and J_{2b} refer to the nearest neighbor AFM, nearest neighbor FM, next nearest neighbor AFM, and next nearest neighbor FM exchange interaction, respectively.

calculation with an enlarged unit cell containing four Fe atoms, and the experimental z(Te) was used, which well reproduces the observed moment and is consistent with our previous study of Fe arsenides [29].

Figure 1 summarizes spin structures found in the parent materials of arsenide superconductors [Fig. 1(a)] and $Fe_{1+x}Te$ for small x [Fig. 1(b)] [19]. In $Fe_{1+x}Te$, the FM spin stripes are doubled and rotated by 45° with respect to the nonmagnetic unit cell (smallest dotted squares). According to the neutron scattering experiment by Li *et al.* [19], this doubled stripe phase realizes at the smallest possible $x \sim 0.068$, i.e., close to the stoichiometric FeTe ($x = 0$). The J_{1a}, J_{1b}, J_{2a}, and J_{2b} represent the first nearest neighbor AFM, FM, second nearest AFM, and FM interactions, respectively. While the second neighbor coupling is always AFM in arsenides [Fig. 1(a)], both FM and AFM second neighbor couplings exist in FeTe [Fig. 1(b)]. As x increases further, the spin ordering becomes incommensurate at $x \sim 0.141$ and the incommensurate ordering vector depends on x. Importantly this different magnetic structure found in $Fe_{1+x}Te$ cannot be matched with the (π, π) nesting which is common for AFM parent materials of all the arsenide superconductors. The different spin structure found in $Fe_{1+x}Te$ remains as a puzzle because DFT calculation predicts the same Fermi surface topology and the same (π, π) nesting [11].

Figure 2 shows the calculated band dispersions of a typical arsenide material, LaFeAsO [Fig. 2(a)], and FeTe [Fig. 2(b)]. As discussed by Subedi *et al.* [11], the two band structures are similar. The Fe-3d states are dominant around the Fermi level while the anion p bands depicted by "fat" bands are located fairly well below the Fermi level, and the similar band structure around the Fermi level produces the same Fermi surface topology. As a result, the same kind of (π, π) nesting is obtained for FeTe as in the other arsenide materials [11]. Here we focus on the differences found in the electronic structure. First, Te-p bands hybridize with Fe-d at around -2.5 eV along $\Gamma - Z$ line while As-4p is well separated from the Fe-3d states. Different features along $\Gamma - Z$ are also found at energies above the Fermi level. In FeTe, there are significant band crossings at about $+0.3$ eV. Another notable difference exists at around the X point above the Fermi level where the parabolic band along $X - M - \Gamma$ is flattening at about $+0.5$ eV in FeTe. It is also noted that there are no band crossings across the X point in the range of $+0.5 - +1.8$ eV. These differences above the Fermi level suggest that possibly different Fermi surface topology is induced by electron doping as excess Fe atoms appear in stoichiometric FeTe host.

Figure 3 shows the Fermi surface for $Fe_{1+x}Te$ as a function of doping: (a) without doping and (b) doping by 0.5 electrons per formula unit. Figure 3(a) is in good agreement with previous calculation [11] and clearly shows the existence of (π, π) nesting as in the arsenides. The most important feature found in Fig. 3(b) is the square-type topology developed at around Γ and $(\pi, 0)$ points with

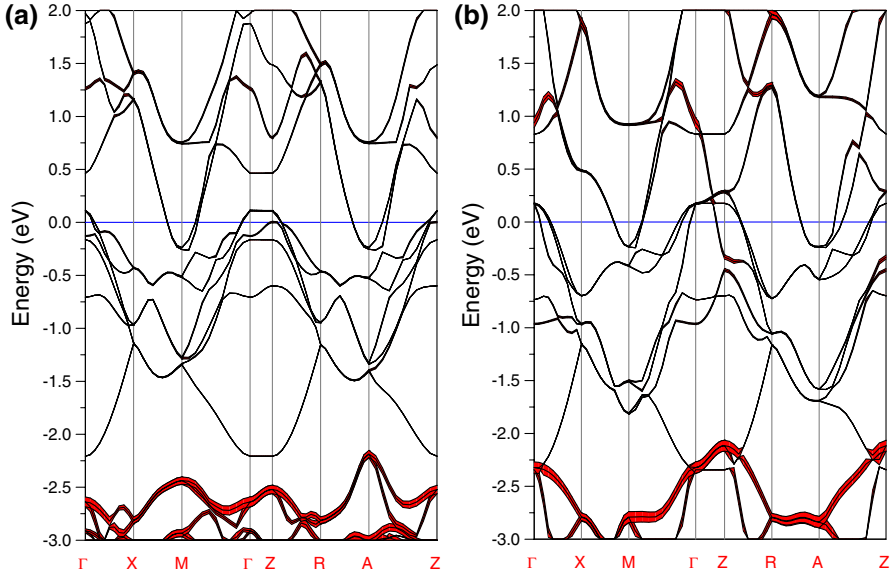

FIG. 2 (color online). The calculated band structure for the nonmagnetic phase of (a) LaFeAsO and (b) FeTe. The As-4p and Te-5p bands are depicted by fat bands. Fermi level is set to be zero (horizontal line).

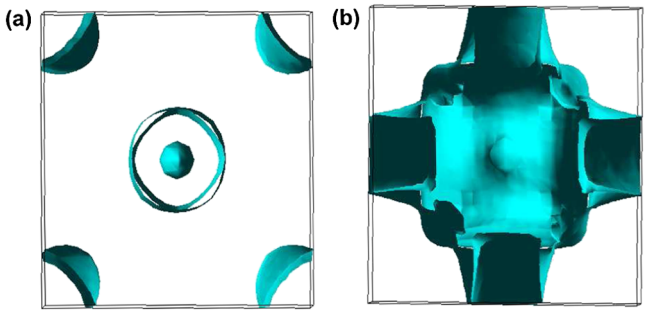

FIG. 3 (color online). Fermi surface (in a-b plane) for FeTe as a function of doping level, δ: (a) $\delta \sim 0.0$, (b) $\delta \sim 0.5$ electron per formula unit. The corner and center of the square unit cell corresponds to the Γ and M point, respectively.

a similar size. It suggests a new nesting at $(\pi, 0)$, which is consistent with the rotated and doubled stripe spin structure [Fig. 1(b)]. The doping level by $\delta \sim 0.5$ electrons would correspond to $Fe_{1.063}Te$ provided all eight valence electrons of excess Fe atoms contribute to the change in the Fermi level within a simple rigid-band approximation. According to a recent neutron scattering by Li *et al.*, the commensurate doubled stripe [Fig. 1(b)] spin structure is realized [19] in $Fe_{1.068}Te$ which is very close to our case. Such agreement assumes that our simplified rigid-band treatment of doping may indeed capture the essential physics of this system.

The nesting property is further examined by calculating the Stoner response function, χ_0, given by

$$\chi_0 = \frac{f(\epsilon_{\mathbf{k}}) - f(\epsilon_{\mathbf{k}+\mathbf{q}})}{\epsilon(\mathbf{k}) - \epsilon(\mathbf{k}+\mathbf{q}) - \omega - i\delta}. \quad (1)$$

Figure 4(a) shows the imaginary part of $\chi_0(\mathbf{q}_z = 0)$ for the stoichiometric FeTe without doping (no excess Fe) in which the (π, π) nesting is clearly seen and is consistent with its Fermi surface in Fig. 3(a). The $\mathrm{Im}\chi_0(\mathbf{q}_z = 0)$ for $\delta = 0.5$ (equivalent to $Fe_{1.063}Te$) is shown in Fig. 4(b). Note the strong $(\pi, 0)$ nesting and the suppressed (π, π) nesting, which demonstrates the remarkable difference of the doped FeTe from the undoped FeTe and Fe arsednies. The novel $(\pi, 0)$ nesting is derived from the square-type Fermi surfaces shown in Fig. 3(b) and is driven by the electron doping through the excess Fe atoms. It is noted that the small amount of excess Fe plays the key role in determining the magnetic structure as the result of the Fermi surface change. Since this $(\pi, 0)$ nesting matches with the rotated-doubled spin stripe found in experiment, our result strongly supports the same spin fluctuation mechanism for superconductivity in Fe chalcogenides as in the Fe arsenides.

The nesting property of $Fe_{1.063}Te$ at $\mathbf{q}_z \neq 0$, is different from that at $\mathbf{q}_z = 0$. While any notable peak is not found in $\mathrm{Im}\chi(\mathbf{q}_z \neq 0)$ for the stoichiometric undoped FeTe, the $\mathrm{Im}\chi_0(\mathbf{q}_z \neq 0)$ of $Fe_{1.063}Te$ shows rather complicated features including both (π, π) and $(\pi, 0)$ peaks with reduced intensities. These features are attributed to a significant variation of the Fermi surface along the Z direction which is also reflected in the band dispersion in Fig. 2. The doping level of $\delta \sim 0.5$ corresponds to the Fermi level shifted by about 0.76 eV where it can be noted that the FeTe bands along $\Gamma - Z$ direction around $\sim +0.76$ eV region are different from those of LaFeAsO (Fig. 2).

By further dopings, the Fermi surface topology once again changes significantly, and the $(\pi, 0)$ nesting disappears. At the doping level of $\delta \sim 1.1$, which would correspond in our analysis to $Fe_{1.141}Te$ with the incommensurate spin order as observed in the experiment [19], the $(\pi, 0)$ nesting is largely suppressed. At this doping level, square-type structures are no longer found in the Fermi surface, and the complicated multiple-peak structure is found to be developed in the χ_0 plot. It might be responsible for the experimentally observed incommensurate spin orderings [15,19]. While, at $\mathbf{q}_z = 0$, neither (π, π) nor $(\pi, 0)$ peak is found in χ_0, several prominent peaks exist at around Γ point which are gradually suppressed along the (π, π) line. At $\mathbf{q}_z = 2\pi/3c$, notable four peaks are found around the (π, π) points. This structure found at $\mathbf{q}_z \neq 0$ shows another difference of $Fe_{1+x}Te$ from FeAs materials and is originated from the different band structures and hybridizations around Z point above the Fermi level as shown in Fig. 2. The accounting for the excess Fe atoms and the validity of the rigid-band approximation is a highly nontrivial prob-

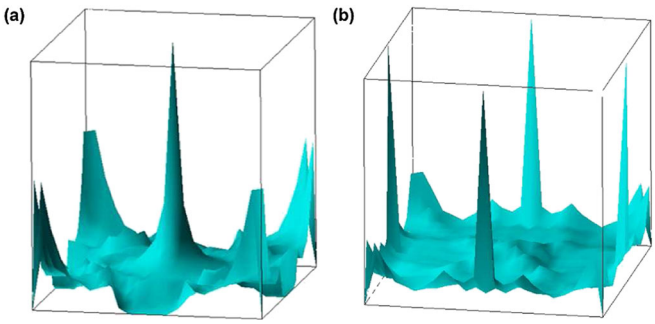

FIG. 4 (color online). The imaginary part of calculated Stoner susceptibility, $\chi_0(\mathbf{q}_z = 0)$, for FeTe in arbitrary unit: (a) $\delta \sim 0.0$, (b) $\delta \sim 0.5$ electron per formula unit.

TABLE I. The calculated Fe moment (in μ_B) and exchange parameters (in meV) for double-stripe $Fe_{1.068}Te$ (doped) and FeTe (undoped) along with the single stripe FeTe (undoped). The results of LaFeAsO are also presented for comparison and the experimental moments are given in parenthesis.

	System	Moment	J_{1a}	J_{1b}	J_{2a}	J_{2b}
Double-stripe	$Fe_{1.068}Te$	2.09 (1.97[b])	−7.6	−26.5	46.5	−34.9
	FeTe	2.16	−4.2	12.9	−6.2	−15.3
Single-stripe	FeTe	2.09	38.6	21.7	5.0	···
	LaFeAsO[a]	1.69 (0.36[c])	47.4	−6.9	22.4	···

[a]Ref. [29].
[b]Ref. [19].
[c]Ref. [30].

lem even when we tried to simulate the doping by supercell calculations. For the present study, however, our excellent agreement with experiment demonstrates that our simplified treatment well describes this material.

The magnetic properties are summarized in Table I. Note that the calculated magnetic moment based on the experimental z(Te) is about 2.09 μ_B which is in good agreement with the neutron data $\sim$1.97 μ_B. This result demonstrates another difference between FeTe and Fe arsenides. In the arsenides, it is known that using experimental z(As) in the calculation always leads to overestimating the Fe moment [29,31,32]. For comparison, we also present in Table I the data for parent material, LaFeAsO. The numbers in parenthesis are the experimental ones. The overestimation by LSDA is more than a factor of 4, which is exceptionally large. The origin of this large discrepancy is still under debate [31]. If the small moment observed in experiment is attributed to domain motions as suggested by Mazin and Johannes [33], the good agreement found in FeTe implies that this system is free from such dynamics, which calls the further investigation along this line.

Table I also shows the calculated exchange couplings of the Heisenberg spin Hamiltonian, $H = J\sum_{\langle i,j\rangle}\mathbf{S}_i \cdot \mathbf{S}_j$, in FeTe compared to the arsenides. Importantly, without doping, even on top of the double-stripe spin ordering, our linear response calculations predict the unstable magnetic interactions. While the charge density self-consistency is achieved for both single- and double-stripe spin order, the spin waves for the undoped FeTe are found to be unstable with respect to the spin angle tilting. For the single-striped FeTe, J_{1b} becomes AFM and its strength is much larger than J_{2a} which is in a sharp disagreement with the single-stripe-stabilized LaFeAsO. In the undoped double stripe FeTe, the overall size of exchange interactions is small, and the signs of J_{1a}, J_{1b}, J_{2a} do not correspond to the actual ordering. It implies that the stoichiometric FeTe ($x = 0.0$) is hardly stabilized, which partly explains the reason that the FeTe sample always has some amounts of excess Fe atoms [19].

The spin waves and magnetic interactions are stabilized in $Fe_{1.063}Te$ being consistent with experiment. In arsenides, the exchange interactions are represented by two major AFM interactions, J_{1a} and J_2, and their strengths are in the same range as is seen in the entire arsenide family [29]: The $J_{1a} \sim 45$ meV and $J_2 \sim 20$ meV while the ferromagnetic J_{1b} is very small. Based on these exchange interactions, the striped AFM phase is stabilized. In $Fe_{1.063}Te$, on the other hand, J_{2a} is the strongest while J_{1a} is as small as J_{1b} in the arsenides. It is noted that the two FM coupling, J_{1b} and J_{2b}, are fairly large which might be responsible for the novel doubled stripe AFM spin order. Our results suggest the spin wave velocities and dispersions for Fe chalcogenides are different from the arsenides, which can be verified by inelastic neutron scattering.

In conclusion, our electronic structure calculations show that a small amount of excess Fe atoms existing in the $Fe_{1+x}Te$ samples changes the Fermi surface topology significantly. As a result, a novel $(\pi, 0)$ nesting appears at $x \approx 0.063$, and the rotated double-stripe AFM spin structure stabilizes. This is different from Fe arsenide parent materials. Our finding of the "missing nesting" explains the origin of the spin density wave observed by a recent neutron experiment and validates the spin fluctuation theory of superconductivity for Fe chalcogenides. The calculated exchange interactions and spin moment demonstrate the role of excess Fe atoms in stabilizing the magnetic structure, and imply a different magnetic behavior of chalcogenide superconductors from the arsenides.

This work is supported by NSF Grant DMR-0606498, and DOE SciDAC Grant SE-FC0206ER25793.

[1] Y. Kamihara *et al.*, J. Am. Chem. Soc. **130**, 3296 (2008).
[2] Z.-A. Ren *et al.*, Chin. Phys. Lett. **25**, 2215 (2008).
[3] M. Rotter, M. Tegel, and D. Johrendt, Phys. Rev. Lett. **101**, 107006 (2008).
[4] J. H. Tapp *et al.*, Phys. Rev. B **78**, 060505(R) (2008).
[5] F.-C. Hsu *et al.*, Proc. Natl. Acad. Sci. U.S.A. **105**, 14 262 (2008).
[6] V. Cvetkovic and Z. Tesanovic, Europhys. Lett. **85**, 37 002 (2009).
[7] I. I. Mazin *et al.*, Phys. Rev. Lett. **101**, 057003 (2008).
[8] D. J. Singh, Physica (Amsterdam) **469C**, 418 (2009).
[9] I. I. Mazin and J. Schmalian, arXiv:0901.4790.
[10] D. J. Singh, Phys. Rev. B **78**, 094511 (2008).
[11] A. Subedi *et al.*, Phys. Rev. B **78**, 134514 (2008).
[12] Y. Mizuguchi *et al.*, Appl. Phys. Lett. **93**, 152505 (2008).
[13] M. H. Fang *et al.*, Phys. Rev. B **78**, 224503 (2008).
[14] K.-W. Yeh *et al.*, Europhys. Lett. **84**, 37 002 (2008).
[15] W. Bao *et al.*, Phys. Rev. Lett. **102**, 247001 (2009).
[16] Y. Mizuguchi *et al.*, arXiv:0810.5191.
[17] Y. Mizuguchi *et al.*, Appl. Phys. Lett. **94**, 012503 (2009).
[18] Y. Mizuguchi *et al.*, arXiv:0811.1123.
[19] S. Li *et al.*, Phys. Rev. B **79**, 054503 (2009).
[20] Y. Xia *et al.*, arXiv:0901.1299 [Phys. Rev. Lett. (to be published)].
[21] T. M. McQueen *et al.*, Phys. Rev. B **79**, 014522 (2009).
[22] C. Fang, B. A. Bernevig, and J. Hu, arXiv:0811.1294.
[23] For a review, see, e.g., *Theory of the Inhomogeneous Electron Gas*, edited by S. Lundqvist and S. H. March (Plenum, New York, 1983).
[24] S. Y. Savrasov, Phys. Rev. B **54**, 16 470 (1996).
[25] A. I. Liechtenstein *et al.*, J. Magn. Magn. Mater. **67**, 65 (1987).
[26] P. Bruno, Phys. Rev. Lett. **90**, 087205 (2003).
[27] X. Wan, Q. Yin, and S. Y. Savrasov, Phys. Rev. Lett. **97**, 266403 (2006).
[28] M. J. Han, X. Wan, and S. Y. Savrasov, Phys. Rev. B **78**, 060401(R) (2008).
[29] M. J. Han *et al.*, Phys. Rev. Lett. **102**, 107003 (2009).
[30] C. de la Cruz *et al.*, Nature (London) **453**, 899 (2008).
[31] I. I. Mazin *et al.*, Phys. Rev. B **78**, 085104 (2008).
[32] Z. P. Yin *et al.*, Phys. Rev. Lett. **101**, 047001 (2008).
[33] I. I. Mazin and M. D. Johannes, Nature Phys. **5**, 141 (2009).